PROCEEDINGS OF SCIENCE

SM $t\bar{t}$ cross section

Prakash Mathews[*†]
Saha Institute of Nuclear Physics
1/AF Bidhan Nagar
Kolkata 700 064, INDIA
E-mail: prakash.mathews@saha.ac.in

An overview of some of the recent theoretical developments that has been made in the top quark pair production at hadron colliders is presented. NNLO corrections to inclusive stable top-quark pair production has now been extended to fully differential distributions, which is exact and complete. Phenomenological implications of precision measurements at the LHC and precise theoretical predictions, *viz.* NNLO total and differential distributions of stable top-quark pair production, are discussed.

9th International Workshop on the CKM Unitarity Triangle
28 November - 3 December 2016
Tata Institute for Fundamental Research (TIFR), Mumbai, India

[*]Speaker.
[†]A footnote may follow.

PoS(CKM2016)116

Top quark is the most massive elementary particle in the Standard Model (SM) and is produced in hadron colliders as top-antitop ($t\bar{t}$) pairs. Top quark is the only quark that decays before hadronisation and hence gives direct access to its properties. Stability of electroweak vacuum when extrapolated to the Planck scale leads to a condition on the Higgs quartic coupling $\lambda(M_P) \geq 0$. To next-to-next-to-leading order (NNLO), this relates the masses of Higgs boson m_h, top quark m_t and the strong coupling α_s [1, 2]. Precise determination of these SM parameters are crucial to infer the fate of the universe.

At the LHC, $t\bar{t}$ inclusive cross section and differential distributions have been very precisely measured [3, 4]. Top-antitop pair production in a hadron collider is the first NNLO computation which is exact (no approximations) and complete (all the sub-processes included), involving the production of two massive, colored fermions. The subprocess that contribute to NNLO (a) $q\bar{q} \to t\bar{t}\, X_2$ [5]; (b) $qq \to t\bar{t}\, X_2$, $qq' \to t\bar{t}\, X_2$, $q\bar{q}' \to t\bar{t}\, X_2$ [6]; (c) $q(\bar{q})g \to t\bar{t}\, X_2$ [7]; (d) $gg \to t\bar{t}\, X_2$ [8], where X_2 denotes two additional partons in the final state. The gg-channel dominants at the LHC while at the Tevatron the $q\bar{q}$-channel dominates. Theoretical predictions are hence available at the full NNLO and including next-to-next-to-leading logarithmic (NNLL) accuracy for total inclusive cross section for stable top.

To estimate the theoretical uncertainties as a result of truncation of the perturbative order, it is standard practice to vary the factorisation scale μ_F and the renormalisation scale μ_R about a central value μ_0. The scale variation of the higher order is well contained with in the scale variations

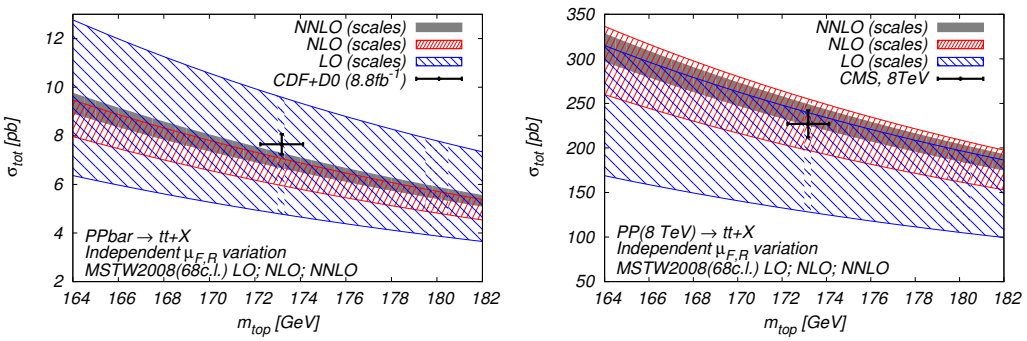

Figure 1: Scale variation of NNLO (black), NLO (red) and LO (blue), total cross-section as a function of top mass at (from [9]) the Tevatron (left) and the LHC 8 TeV (right). Experimental measurements are shown.

of subsequent lower orders as can be see in Fig. 1 for NNLO, NLO and LO— indicates that the scale variation approximates the missing higher order terms pretty well [9]. Scale dependence for various fixed order and logarithmic accuracy is plotted in Fig. 2. PDF sets, match the accuracy of the fixed order. Impact of soft-gluon resummation on the size of the scale dependence and the theoretical central value, is shown in Fig. 2. Inclusion of resummation with logarithmic accuracy decreases the scale dependence. Perturbative convergence is preserved after the inclusion of soft-gluon resummation [9].

Top-quark pair production at the LHC is directly sensitive to large-x gluon PDF (between $x = 0.1$ and $x = 0.5$) where the uncertainties are relatively large for gluon [10]. The NNLO computation of the total $t\bar{t}$ cross section, made it possible for the inclusion of precise data from the Tevatron and

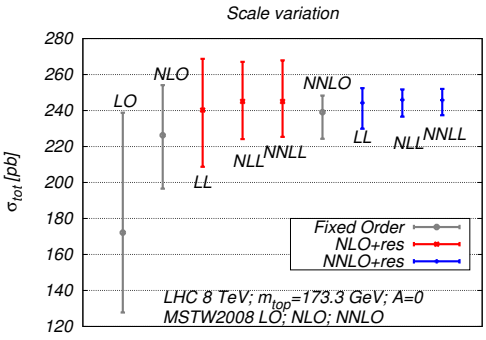

Figure 2: For 8 TeV LHC, the scale uncertainty of the predicted total cross section at fixed order LO, NLO and NNLO (grey). Further the soft-gluon resummation at LL, NLL and NNLL have been included to the fixed order NLO and NNLO (from [9]).

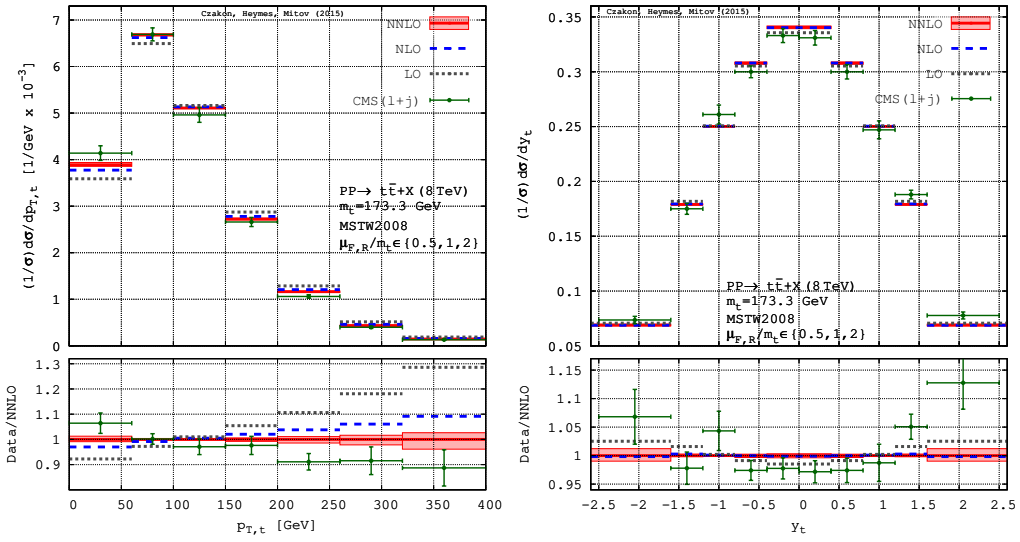

Figure 3: Transverse momentum and rapidity distribution of the average of top and antitop quark distribution. Scale variation is only shown for the NNLO correction [11].

LHC into a NNLO global PDF analysis. Improvement in the PDF uncertainties in the large-x region will have an impact on predictions for BSM particle production which are initiated by gluons at the LHC. With substantial reduction in scale uncertainties of the NNLO results, the main uncertainties: scale, PDFs and top quark mass, are all in the same ballpark region of around 2-3%.

Fully differential distributions for stable top-quark pair production to NNLO in QCD is now available [11, 12]. It was essential to account for the difference between the SM prediction of the p_T spectrum of stable tops and the LHC measurements on top-quark p_T distribution, obtained by unfolding to the stable top-quark distribution (on account of the fact that top quarks are not measured directly, but inferred from its decay products). Though there could be other sources to account for this difference, it was important to include more terms in the perturbative QCD

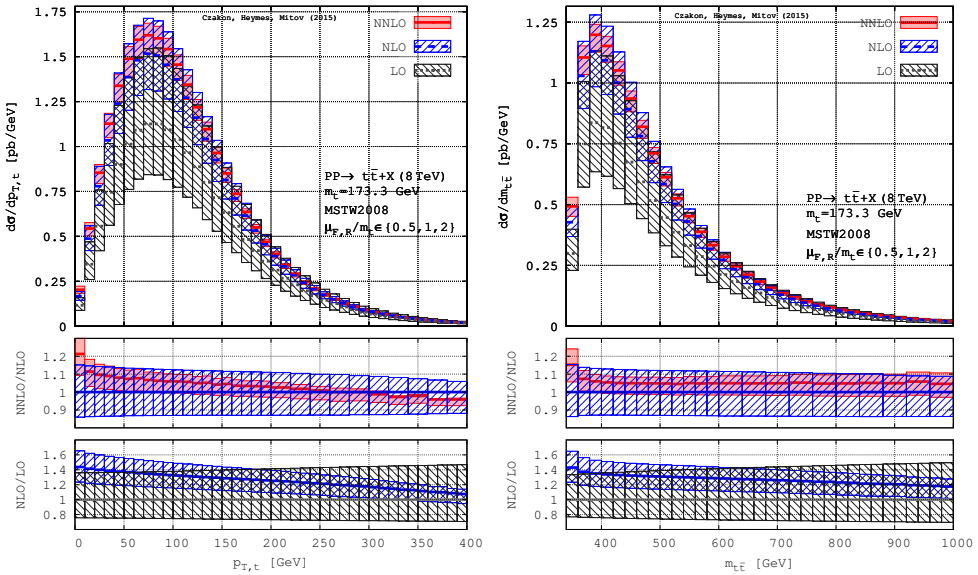

Figure 4: LO, NLO, NNLO p_T of t or $\bar{t}$ distribution (left) and invariant mass of top pair (right) [11].

expansion.

Normalised $p_{T,t}$ distribution at LO, NLO, NNLO is compared to CMS data [4] in Fig. 3 (left panel) and normalised rapidity y_t distribution (right panel). Including the NNLO QCD contribution in the $p_{T,t}$ distribution gets the SM prediction closer to the CMS data in all bins. As a check, the NNLO distributions were used to reproduce the NNLO inclusive cross section for particular values of μ_R and μ_F and the cancellation of IR singularities were also verified.

In Fig. 4, scale variation of LO, NLO and NNLO is plotted for top-antitop p_T distribution (left panel) and $m_{t\bar{t}}$ (right panel). The lower insets also includes the NLO and NNLO K-factors. The scale variation shows the consistent pattern of reduction of scale variation with inclusion of successive higher order terms. This computation includes all partonic channel contributions to NNLO and does not resort to leading color approximation, but in order to compare with the NNLO total cross section a fixed scales have been used for the differential distribution. More natural to have used a dynamical scale, *viz.* $m_T = \sqrt{m_t^2 + p_T^2}$ which would deviate from the fixed scale at large p_T.

The choice of an appropriate central value μ_0 about which the variation of scale is done, need to be addressed and the guiding principle have been to look for minimum sensitivity and faster perturbative convergence [13]. For stable $t\bar{t}$ total cross section the natural choice is $\mu_0 \sim m_t$, but the scale at which perturbative convergence is maximal is slightly above $m_t/2$, significantly lower than the standard choice $\mu_0 = m_t$ (see Fig. 5). Other possible choice of μ_0 that could be relevant for differential distribution are:

$$m_T = \sqrt{m_t^2 + p_T^2}\,; \qquad H_T = \sqrt{m_t^2 + p_{T,t}^2} + \sqrt{m_t^2 + p_{T,\bar{t}}^2}\,; \qquad E_T = \sqrt{\sqrt{m_t^2 + p_{T,t}^2}\sqrt{m_t^2 + p_{T,\bar{t}}^2}}\,;$$

$$H_T' = \sqrt{m_t^2 + p_{T,t}^2} + \sqrt{m_t^2 + p_{T,\bar{t}}^2} + \sum_i p_{T,i}\,; \quad H_{T,\mathrm{int}} = \sqrt{(m_t/2)^2 + p_{T,t}^2} + \sqrt{(m_t/2)^2 + p_{T,\bar{t}}^2}\,; \quad m_{t\bar{t}}\,.$$

Apart from the above functional form of μ_0, the proportionality constant also needs to be fixed. Predictions are stable with respect to the choice of PDF sets at NNLO level (Fig. 5) for different

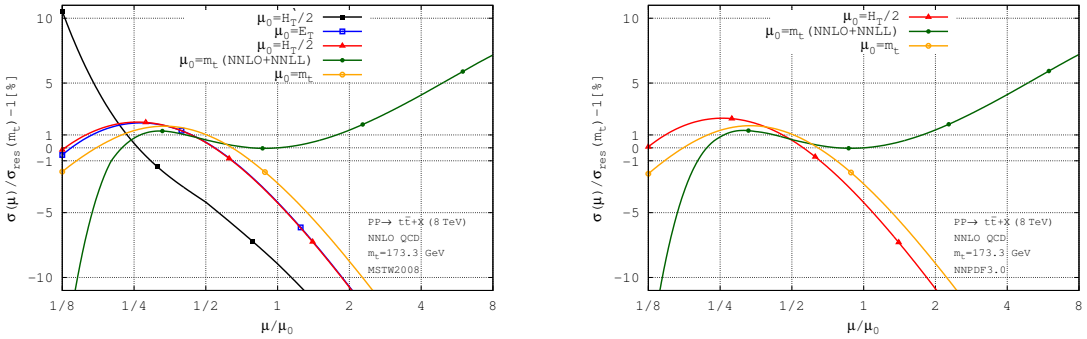

Figure 5: Total cross section at NNLO is compared for two PDF sets and different dynamical scales. Each curve is normalised to the NNLO+NNLL resumed cross section at the scale $\mu_0 = m_t$ [13].

dynamical scales. Scale variation around $\mu/\mu_0 = 1/2$ is regular and monotonic, hence faster perturbative convergence and sensitivity is minimal, except for the dynamical scale $\mu_0 = H'_T/2$ (see Fig. 5 left panel).

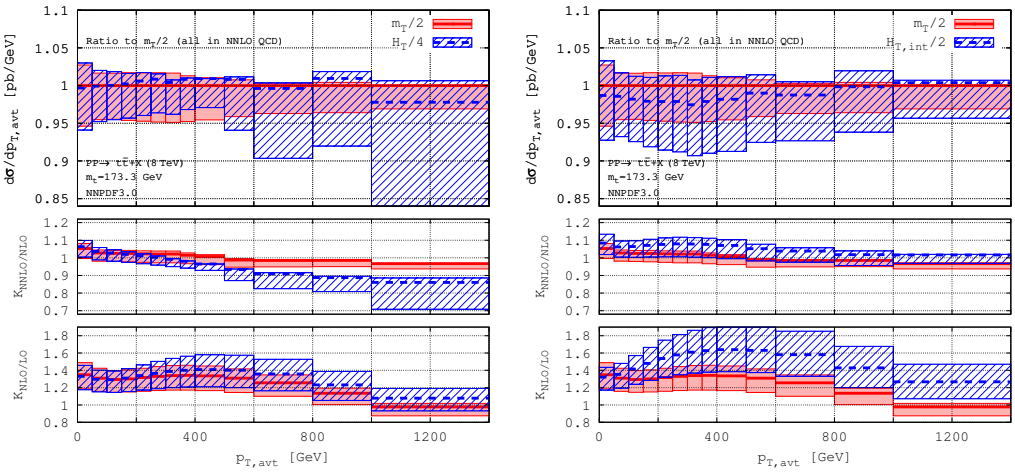

Figure 6: The ratio of average top/antitop p_T distribution at NNLO for dynamical scale $H_T/4$ (left) and $H_{T,int}/2$ (right) with respect to $m_T/2$. The corresponding NLO and NNLO, K-factor are shown as lower insets [13]

The scale choices $H_T/4$ and $m_T/2$ have the same behavior in the limits $p_{T,t} \to 0$ and $p_{T,t} \to \infty$. As the limit $p_{T,t} \to 0$ is related to the total cross section, behavior in this region could be guided by σ_{tot}. For the large $p_{T,t}$ case, as the data is not sufficient to constrain this region, the principle of fastest perturbative convergence has been used [13]. In Fig. 6 for $p_{T,t}$ distribution, dynamical scale $H_T/4$ and $H_{T,int}/2$ has been compared to $m_T/2$ by taking the ratio and scale variation gives the band. It is seen that for $p_{T,t}$ distribution, dynamical scale $m_T/2$ is least sensitive to scale variation. Further the NNLO K-factor is closer to unity compared to the NLO K-factor and scale variation spread is smaller for $m_T/2$ compared to $H_T/4$ and $H_{T,int}/2$; demonstrates fastest perturbative con-

vergence in the full kinematical range. The most appropriate scale for p_T distribution is hence $m_T/2$ and for the other distributions $H_T/4$ [13].

With large number of top quark pairs produced at the LHC and high precision computation at NNLO+NNLL for the total inclusive top-pair production and NNLO differential distribution, top physics has entered a high precision phase. This would facilitate high precision phenomenological studies *viz.* direct measurement of running α_s at high scale to NNLO accuracy, extraction of NNLO PDFs from LHC data. Precise determination of α_s is essential to reduce theoretical uncertainties for any high-precision pQCD observables that depends on higher powers of α_s. Using the fully differential calculation of the NNLO QCD corrections to inclusive top pair production, the next higher order contribution to top quark forward-backward asymmetry was determined [14] and was found to be large, substantial enough to bring the value closer to the D0 [15] and CDF [16] measurements. Impact of precision measurements of differential distributions of top-quark pair by ATLAS [3] and CMS [4] at $\sqrt{s} = 8$ TeV, on PDFs have recently been studied [17] using the NNLO theoretical prediction. Differential distributions provide significant constraints on large-x gluon which are comparable to those obtained from inclusive jet production data. An important ingredient for future global PDF fits.

References

[1] G. Degrassi, S. Di Vita, J. Elias-Miro, J. R. Espinosa, G. F. Giudice, G. Isidori and A. Strumia, JHEP **1208** (2012) 098.

[2] F. Bezrukov, M. Y. Kalmykov, B. A. Kniehl and M. Shaposhnikov, JHEP **1210** (2012) 140.

[3] G. Aad *et al.* [ATLAS Collaboration], Eur. Phys. J. C **76** (2016) no.10, 538.

[4] V. Khachatryan *et al.* [CMS Collaboration], Eur. Phys. J. C **75** (2015) no.11, 542.

[5] P. Bärnreuther, M. Czakon and A. Mitov, Phys. Rev. Lett. **109** (2012) 132001.

[6] M. Czakon and A. Mitov, JHEP **1212** (2012) 054.

[7] M. Czakon and A. Mitov, JHEP **1301** (2013) 080.

[8] M. Czakon, P. Fiedler and A. Mitov, Phys. Rev. Lett. **110** (2013) 252004.

[9] M. Czakon, P. Fiedler, A. Mitov and J. Rojo, arXiv:1305.3892 [hep-ph].

[10] M. Czakon, M. L. Mangano, A. Mitov and J. Rojo, JHEP **1307** (2013) 167.

[11] M. Czakon, D. Heymes and A. Mitov, Phys. Rev. Lett. **116** (2016) no.8, 082003.

[12] M. Czakon, P. Fiedler, D. Heymes and A. Mitov, JHEP **1605** (2016) 034.

[13] M. Czakon, D. Heymes and A. Mitov, arXiv:1606.03350 [hep-ph].

[14] M. Czakon, P. Fiedler and A. Mitov, Phys. Rev. Lett. **115** (2015) no.5, 052001.

[15] V. M. Abazov *et al.* [D0 Collaboration], Phys. Rev. D **90** (2014) 072011.

[16] T. Aaltonen *et al.* [CDF Collaboration], Phys. Rev. D **87** (2013) no.9, 092002.

[17] M. Czakon, N. P. Hartland, A. Mitov, E. R. Nocera and J. Rojo, arXiv:1611.08609 [hep-ph].